

NASA/TM-2002-211778



# Hypersonic Shock Interactions About a $25^\circ/65^\circ$ Sharp Double Cone

*James N. Moss*  
*Langley Research Center, Hampton, Virginia*

*Gerald J. LeBeau*  
*Johnson Space Center, Houston, Texas*

*Christopher E. Glass*  
*Langley Research Center, Hampton, Virginia*

---

August 2002

## The NASA STI Program Office ... in Profile

Since its founding, NASA has been dedicated to the advancement of aeronautics and space science. The NASA Scientific and Technical Information (STI) Program Office plays a key part in helping NASA maintain this important role.

The NASA STI Program Office is operated by Langley Research Center, the lead center for NASA's scientific and technical information. The NASA STI Program Office provides access to the NASA STI Database, the largest collection of aeronautical and space science STI in the world. The Program Office is also NASA's institutional mechanism for disseminating the results of its research and development activities. These results are published by NASA in the NASA STI Report Series, which includes the following report types:

- **TECHNICAL PUBLICATION.** Reports of completed research or a major significant phase of research that present the results of NASA programs and include extensive data or theoretical analysis. Includes compilations of significant scientific and technical data and information deemed to be of continuing reference value. NASA counterpart of peer-reviewed formal professional papers, but having less stringent limitations on manuscript length and extent of graphic presentations.
- **TECHNICAL MEMORANDUM.** Scientific and technical findings that are preliminary or of specialized interest, e.g., quick release reports, working papers, and bibliographies that contain minimal annotation. Does not contain extensive analysis.
- **CONTRACTOR REPORT.** Scientific and technical findings by NASA-sponsored contractors and grantees.
- **CONFERENCE PUBLICATION.** Collected papers from scientific and technical conferences, symposia, seminars, or other meetings sponsored or co-sponsored by NASA.
- **SPECIAL PUBLICATION.** Scientific, technical, or historical information from NASA programs, projects, and missions, often concerned with subjects having substantial public interest.
- **TECHNICAL TRANSLATION.** English-language translations of foreign scientific and technical material pertinent to NASA's mission.

Specialized services that complement the STI Program Office's diverse offerings include creating custom thesauri, building customized databases, organizing and publishing research results ... even providing videos.

For more information about the NASA STI Program Office, see the following:

- Access the NASA STI Program Home Page at **<http://www.sti.nasa.gov>**
- E-mail your question via the Internet to **[help@sti.nasa.gov](mailto:help@sti.nasa.gov)**
- Fax your question to the NASA STI Help Desk at (301) 621-0134
- Phone the NASA STI Help Desk at (301) 621-0390
- Write to:  
NASA STI Help Desk  
NASA Center for Aerospace Information  
7121 Standard Drive  
Hanover, MD 21076-1320

NASA/TM-2002-211778



# Hypersonic Shock Interactions About a $25^\circ/65^\circ$ Sharp Double Cone

*James N. Moss*  
*Langley Research Center, Hampton, Virginia*

*Gerald J. LeBeau*  
*Johnson Space Center, Houston, Texas*

*Christopher E. Glass*  
*Langley Research Center, Hampton, Virginia*

National Aeronautics and  
Space Administration

Langley Research Center  
Hampton, Virginia 23681-2199

---

August 2002

---

Available from:

NASA Center for AeroSpace Information (CASI)  
7121 Standard Drive  
Hanover, MD 21076-1320  
(301) 621-0390

National Technical Information Service (NTIS)  
5285 Port Royal Road  
Springfield, VA 22161-2171  
(703) 605-6000

# Hypersonic Shock Interactions About a $25^\circ/65^\circ$ Sharp Double Cone

James N. Moss\*, Gerald J. LeBeau†, and Christopher E. Glass\*

*\*NASA Langley Research Center, MS 408A, Hampton, VA 23681-2199*

*†NASA Johnson Space Center, EG3, Houston, TX 77058-3696*

**Abstract.** This paper presents the results of a numerical study of shock interactions resulting from Mach 10 air flow about a sharp double cone. Computations are made with the direct simulation Monte Carlo (DSMC) method by using two different codes: the G2 code of Bird and the DAC (DSMC Analysis Code) code of LeBeau. The flow conditions are the pretest nominal free-stream conditions specified for the ONERA R5Ch low-density wind tunnel. The focus is on the sensitivity of the interactions to grid resolution while providing information concerning the flow structure and surface results for the extent of separation, heating, pressure, and skin friction.

## INTRODUCTION

Shock/shock and shock/boundary layer interactions continue to receive considerable attention because of their impact on the performance and design requirements of hypersonic vehicles. Developing an experimental database from a broad range of ground-based test facilities is a key element in providing the basis for assessing the practicality and accuracy with which various computational methods can be applied for such complex flows. Recent [1] and proposed [2] experiments along with computational studies are providing such information for relatively low Reynolds number conditions. The recent experiments conducted by Calspan-University at Buffalo Research Center (CUBRC) personnel [1] provide a substantial database for  $25^\circ/55^\circ$  double cones, both sharp and blunted, where the experiments were performed in hypersonic shock tunnels. These tests were conducted in nitrogen and included surface measurements for heating and pressure and schlieren imagery at Mach numbers ranging from 9.25 to 11.4. Computations, using both computational fluid dynamic (CFD) and DSMC methods, have been performed for several of the CUBRC experiments, and an initial comparison and assessment of the experimental and computational data was presented in Ref. [3]. Subsequent studies and examination of the original experimental/computational results have identified several significant findings. One finding is that grid resolved DSMC solutions for the CUBRC biconic test conditions are not practical [4], and, consequently, the coarse grid solutions that have been made fail to predict the correct details of the separated region. Yet for the same problems, a number of continuum CFD solutions have provided fair to good agreement with the CUBRC data for the extent of the separated region. A second finding is that both DSMC and CFD solutions can differ substantially (as much as 33 percent, as discussed in Ref. [5]) with the measured heating rates upstream of the separated region, that is, for laminar flow about either sharp [5] or blunted cones [6] at zero incidence. With differences of this magnitude, additional studies were done to understand/define the flow conditions for which the CUBRC measurements were made. Initial results of a reconciliation effort are described in Ref. [7] with a new set of free-stream conditions presented in Ref. [8].

As the reconciliation process evolves for the CUBRC test cases, new experiments are being prepared [2] for a  $25^\circ/65^\circ$  double cone model in a conventional low-density wind tunnel at ONERA (Office National d'Études et de Recherches Aéropatiales). The ONERA tests will be performed in the R5Ch wind tunnel and are the focus of the current computational investigation. The R5Ch flow conditions are more amenable to DSMC simulation but are still very demanding, as is demonstrated in the present study. The ONERA experiments

will be for Mach 10 air flow at a low Reynolds number condition ( $Re_{\infty,d} = 12124$ , where  $d$  is the maximum model diameter). For the double-cone models investigated, the first cone is sharp with a half angle of  $25^\circ$ , while the second cone has a half angle of  $65^\circ$ . This double cone geometry produces strong shock interactions because the attached shock from the first cone interacts with the detached bow shock from the second cone. Also, the outer shocks are modified by the separation and reattachment shocks where the extent of flow separation is significant for the current combination of model size and flow conditions. Results presented emphasize the sensitivity of the surface quantities (heating, pressure, and skin friction) to grid resolution. Future opportunities will exist for comparing the current computational data with the ONERA experiments. These experiments [2] will include surface results from pressure, heating rate, and oil flow measurements and flow visualization from electron beam fluorescence (EBF) measurements. Careful comparisons and analysis of computational and experimental results are essential in establishing confidence in both the data and the computational tools.

The DSMC codes used in the current study are the parallel DAC (DSMC Analysis Code) code of LeBeau [9,10] and the scalar G2 code of Bird [11,12]. Major emphasis will be on the DAC results since the current study indicates that it is not practical (excessive run time) to obtain a grid resolved solution for the current problem with a scalar (single processor) code such as G2.

## DSMC CODES

The DSMC codes used in the current study are the DAC code of LeBeau [9,10], software that provides 3D, 2D, and axisymmetric capabilities, and the general 2D/axisymmetric code of Bird [11,12] (G2). The molecular collisions are simulated with the variable hard sphere (VHS) molecular model. Energy exchange between kinetic and internal modes is controlled by the Larsen-Borgnakke statistical model [13]. For the present study, the simulations are performed by using nonreacting gas models while considering energy exchange between translational, rotational, and vibrational modes. The model surface is assumed to have a specified constant temperature. Full thermal accommodation and diffuse reflection are assumed for the gas-surface interactions.

The DAC code used in the current study makes use of the parallel option and the recently introduced axisymmetric capability [10] of the DAC software. The DAC software gains much of its flexibility and performance by decoupling the grids used to resolve the flow field and surface geometry. The surface geometry is discretized by using an unstructured triangular grid representation, which permits a great deal of boundary condition flexibility on the surface. A two-level embedded Cartesian grid is employed for the flow-field discretization so that flow-field property variations may be handled more efficiently. This gridding strategy also uses the DAC preprocessor software to address the task of creating an appropriate flow-field grid.

The computational domain of the flow field is bounded by user specified limits. This computational domain is divided into a Cartesian network of cells with constant, yet independent spacing in each of the coordinate directions. The cells of this first level of Cartesian discretization are referred to as level-I cells. The resolution of this grid is typically set based on the minimum desired flow-field sampling resolution for a given problem. To further refine the flow-field grid in areas of increased density or high gradients, each level-I cell can have an additional level of embedded Cartesian refinement, level-II cells. This second level of refinement is independent for each level-I cell and is also variable in each of the coordinate directions should refinement in a specific direction be desired. The procedure used in the current study was to do a series of grid refinements/adaptions once an initial solution based on a level-I discretization was obtained. Each refinement is based on computed flow properties of the previous solution and user specified parameters that control (for example, the local cell dimensions are based on local mean free path or local flow gradients) the cell resolution. The achieved cell resolution is usually close to the user specified value throughout the computational domain. By carefully stepping through a series of adaptations, one can identify the sensitivity of the solution to grid resolution and, at the same time, ensure that the grid adaption, local time steps, and cell-simulated molecule populations are based on time-converged values.

For the G2 simulations, the computational domain consisted of an arbitrary number of regions. Each region is subdivided into cells where the collision rate is set by the cell average properties. Also, the cells in selected regions are subdivided into subcells to enhance the spatial resolution used to select collision partners and thereby minimize the loss of angular momentum and viscous transport errors. In general, the cell dimensions within a region were nonuniform in both directions, with geometric stretching exceeding an order of magnitude in some regions. The macroscopic quantities are time-averaged results extracted from the individual cells. Since the computational regions were not run with necessarily the same time step, it was essential that steady state conditions be established before generating the final time-averaged results. Steady state was assumed to

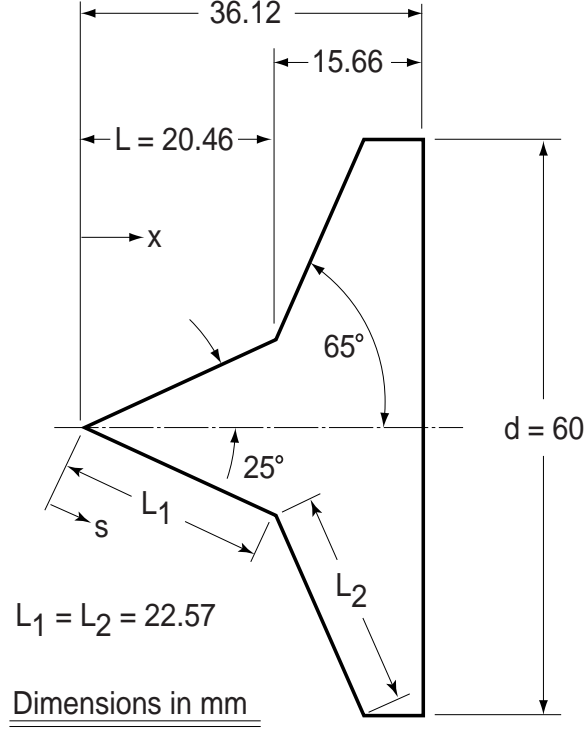


**FIGURE 1.** ONERA sharp double cone model where  $x$  is measured from the vertex.

**TABLE 1.** Nominal pretest free-stream and surface<sup>a</sup> conditions for the ONERA R5Ch tunnel.

$V_\infty$ , m/s	$\rho_\infty \times 10^4$ , kg/m <sup>3</sup>	$n_\infty \times 10^{-22}$ , m <sup>-3</sup>	$T_\infty$ , K	$p_\infty$ , N/m <sup>2</sup>	Gas	$M_\infty$	$Re_{\infty,d}$	$T_w$ , K
1382.6	4.520	0.940	48.5	6.30	Air	9.90	12 124	290.0

<sup>a</sup> Diffuse with full thermal accommodation.

occur when all molecules used in the simulation, the average molecules used in each region, and the surface quantities (locations and size of the separation region, and heating) became essentially constant when they were time averaged over significant time intervals.

## RESULTS OF CALCULATIONS FOR A SHARP DOUBLE CONE

Details of the model configuration that will be used in the ONERA tests are presented in Fig. 1. For this sharp double cone model, the first cone has a half angle of  $25^\circ$  and the second cone has a half angle of  $65^\circ$ . The two cones are the same length (22.57 mm), while the projected length of the first cone on the  $x$ -axis is 20.46 mm. Table 1 provides a summary of the free-stream and surface boundary conditions used in the current study. Information concerning calculated locations and extent of separation are included in Table 2 as a function of grid or cell density for both G2 and DAC simulations. Extent of separation is presented in terms of two measurements: (1) the distance measured along the  $x$ -axis of the model and (2) the wetted distance along the surface  $s$ . The Reynolds number is based on free-stream conditions with a characteristic length  $d$ , the maximum diameter of the model. For the R5Ch flow conditions, the Sutherland viscosity has been used in defining the Reynolds number to be consistent with experimentally reported values.

Two DSMC codes are used in the present study to predict the flow features about a biconic that has significant shock interactions. For the current problem, the solutions obtained with the scalar G2 code used

**TABLE 2.** Results of DSMC calculations for a  $25^\circ/65^\circ$  sharp double cone.

Code	Cells	Subcells	$x_S$ , mm	$x_R$ , mm	$\Delta x/L$	$s_S$ , mm	$s_R$ , mm	$\Delta s/L_1$
G2	38 210	38 210	13.34	22.52	0.449	14.72	27.44	0.564
G2	38 210	543 780	12.45	23.51	0.541	13.74	29.79	0.711
G2	89 850	885 400	12.10	23.78	0.571	13.34	30.42	0.757
G2	181 585	1 788 280	11.86	24.10	0.598	13.09	31.21	0.803
DAC	908 757	—	11.34	24.29	0.633	12.51	31.63	0.847
DAC	846 530	—	10.19	25.40	0.743	11.24	34.26	1.020
DAC	1 574 017	—	9.80	25.85	0.785	10.81	35.33	1.086
DAC	1 613 924	—	9.73	25.89	0.790	10.74	35.42	1.093

high aspect ratio cells (cells whose dimensions are very large in the flow direction compared to the surface normal direction), an approach that reduces the computational requirements and has been successfully applied to many classes of problems free of shock interactions. If one could use a grid resolution such that the cell dimensions are on the order of the local mean free path, the prevailing evidence suggests that the solution would be grid independent. With such a resolution, the computational requirements would be substantially larger, requiring parallel resources to obtain solutions for the more demanding problems. Consequently, the parallel DAC code, with the axisymmetric option, was used to provide a much higher level of grid refinement than is possible with G2.

Table 2 provides the key findings of the present study as to the effect of grid resolution on the calculated extent or size of the separation region. First, the G2 and DAC results show that the calculated separation extent increases with grid refinement, an expected result consistent with previous DSMC simulations for related problems. Second, it was not practical to obtain a grid converged solution using the scalar G2 code, since the run time on a single processor SGI R10000 work station was approximately two months for the finest grid simulation. Third, the DAC results from a series of grid refinement solutions show evidence of achieving or approaching a grid resolved solution. The number of cells for the finest grid DAC solution was almost an order of magnitude greater than that used in the finest grid G2 solution. Even though the finest grid G2 solution had a large number of subcells, about the same as the number of cells in the finest grid DAC solution, the results for the extent of separation are very different from that of the finest grid DAC solution.

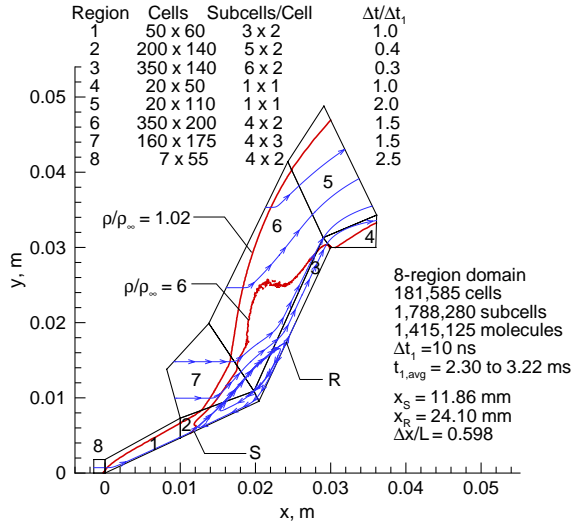


Fig. 2a. G2 parameters and results.

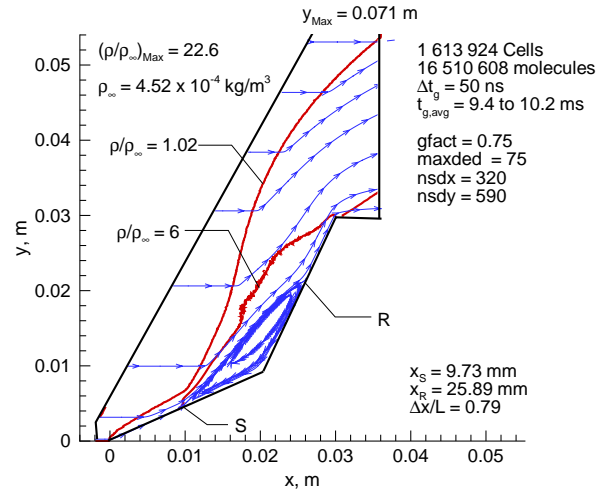


Fig. 2b. DAC parameters and results.

**FIGURE 2.** Finest grid solutions for biconic — computational domain, streamlines, and density contours.

Results presented in Figs. 2 through 4 provide additional insight as to the sensitivity of flow-field and surface results to grid resolution. Figures 2 through 3 present information concerning the computational domain,



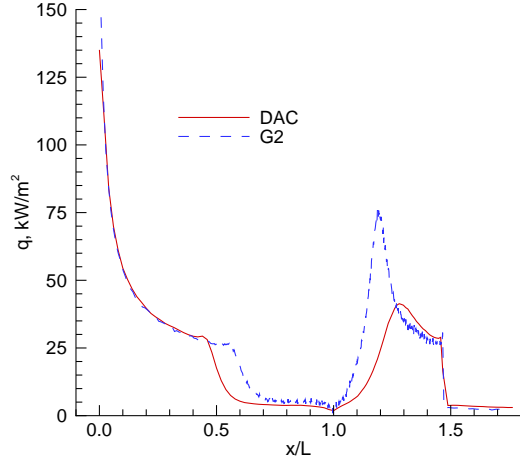


Fig. 3a. Heating rate.

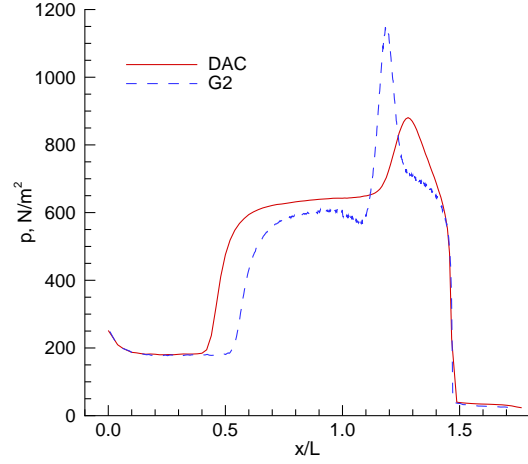


Fig. 3b. Pressure.

**FIGURE 3.** Comparison of surface distribution for the finest grid DAC and G2 solutions.

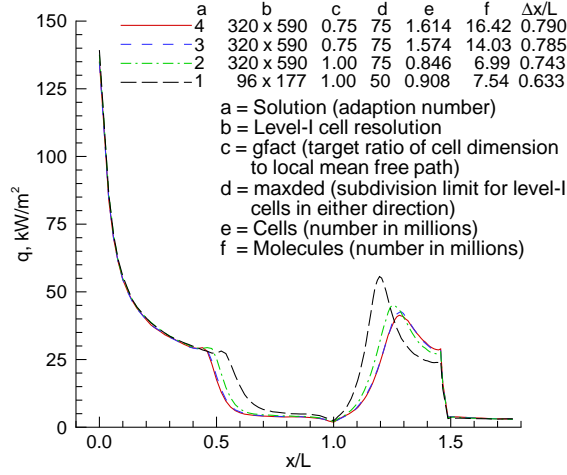


Fig. 4a. Heating rate.

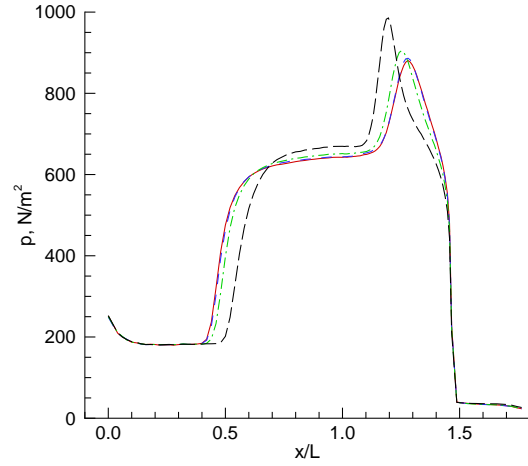


Fig. 4b. Pressure.

**FIGURE 4.** Effect of grid resolution on DAC calculated surface quantities.

solution parameters, and results for the finest grid simulations obtained with each of the two codes. As indicated in Fig. 2a, the G2 computational domain contained eight arbitrary regions, where the computational time step and scaling factor relating real to simulated molecules are constant within a given region. Also included in Fig. 2a are the region time step values ratioed to the region one value along with the number of cells and subcells in each region. The DAC computational domain is described in Fig. 2b, where the upper portion of the domain ends at  $y = 0.071$  m. The number of level-I cells within the computational domain was only a fraction of the user specified number of cells in the  $x$  and  $y$  directions ( $nsdx = 320$  and  $nsdy = 590$ ), since the  $xy$  computational domain is not rectangular. This level-I cell resolution corresponds to a cell resolution of approximately a local mean free path in the undisturbed free stream. The number of level-II

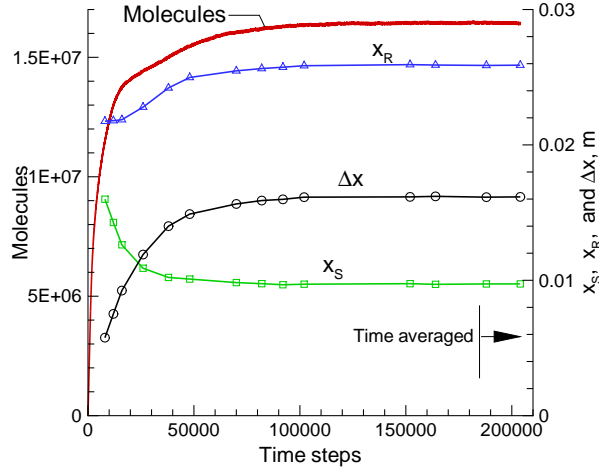


Fig. 5a. Simulation history.

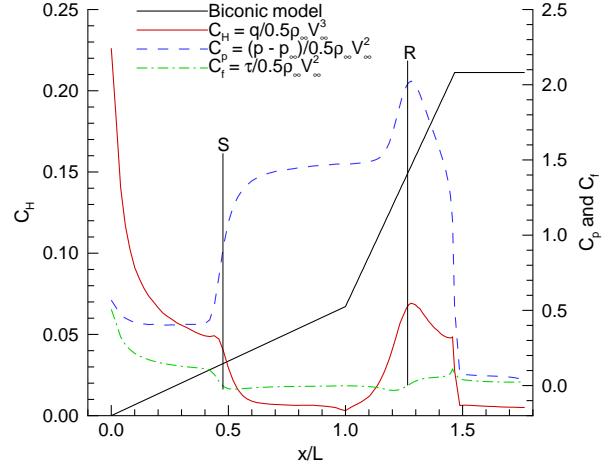


Fig. 5b. Surface coefficients.

**FIGURE 5.** Simulation history and surface coefficient results for finest grid DAC simulation.

cells within each level-I cell is a function of the local flow condition and the user specified parameters *gfact* and *maxded*. The *gfact* parameter is the target resolution of the cell size ratioed to the local mean free path, 0.75 in the present case. The *maxded* parameter serves as a constraint on the number of subdivisions that a level-I cell can be subdivided in either the x or y directions, 75 in the present case. The maximum number of subdivisions any level-I cell experienced for the finest grid simulation was approximately 25 along either the x or y directions; that is, about 625 level-II cells within a given level-I cell. Consequently, a *maxded* of 75 was not a grid constraint in the fine grid simulation.

The general flow-field features are indicated in Fig. 2 where several arbitrary stream lines and two density contours (1.02 and 6.0 times the free-stream value) are shown. The locations for separation and reattachment are indicated by S and R, respectively. The impact of grid resolution is apparent from an examination of the flow-field features, but even more so from the comparison of surface results such as those shown in Fig. 3 for heating and pressure distributions. Upstream of separation, the two solutions are in close agreement with respect to both heating and pressure distributions.

Figures 4 and 5 present results highlighting the DAC simulations. Figures 4a and 4b present the calculated surface heating rate and pressure distributions resulting from four separate simulations, where the grid used in each of the four solutions is inferred or adapted to the results from the previous solution. Results and details for the initial solution using only level-I cells (96 x 177) are not shown because this simulation did not produce a separation region. The present sequential grid adaptions and simulations show that the extent of separation continues to increase with grid refinement and potentially approaches a constant value as a grid resolved simulation is achieved. This later point is not conclusive based on the present simulations since adaption 4 is just a repeat of adaption 3 in terms of the user set parameters; however, the fourth adaption does produce some additional grid refinement and adjustment in the number of simulated molecules. In fact, the present DAC simulations indicate that the number of adaptions to achieve a grid resolved solution is significant for the current problem.

The simulation history for the finest grid solution (Fig. 5a) shows the evolution of the total number of simulated molecules and details concerning the separation region (separation denoted by  $x_S$ , reattachment by  $x_R$ , and the extent of separation by  $\Delta x$ ). The total number of time steps used in this simulation was 204,000, where the time averaged flow-field and surface quantities were extracted from the last 20,000 time steps. The data shown in Fig. 5a suggest that a steady state is achieved at approximately 100,000 time steps; consequently, the current results for the finest grid simulation are time resolved. As indicated in Fig. 2b, the global time step for the present simulation was 50 ns; furthermore, an examination of the contours of the local cell time steps (not shown) shows that the time steps within the shock layer enveloping the biconic have values that are

predominantly in the range of 0.1 to 0.4 of the global value, with the major portion being in the range of 0.1 to 0.2. Additional inspection shows that the individual cells were populated with approximately ten molecules per cell and that the size of the cells in relation to the local mean free path was well aligned with the target value of 0.75. Within the shock layer, the calculated maximum value for the overall kinetic temperature was 942 K, the maximum density was 22.6 times the free-stream value, and the maximum scalar pressure was 141 times the free-stream value. The large separated region (Fig. 2b) has a single vortex embedded in subsonic flow.

Figure 5b presents a summary of the DAC surface results for the finest grid solution in coefficient form (heating, pressure, and skin friction). Also shown is a sketch of the double cone model and vertical lines indicating the locations for separation and reattachment, as inferred from the surface friction distribution (reversal in sign of shear stress). The qualitative features are consistent with experimental trends based on laminar separated flows [14]. First, the separation position (indicated by the vertical line labeled S in Fig. 5b) is in close agreement with the location of the first inflection point (maximum slope) of the initial pressure rise and is also the location at which the heat transfer rate decreases significantly with respect to that for a single pointed cone. Second, the pressure reaches a plateau for a significantly large separation region, while the heat transfer is significantly reduced. Third, at or preceding the intersection of the two cones ( $x/L = 1.0$ ), the heat transfer experiences a minimum and then increases rapidly, as does the pressure, with increasing distance along the second cone. The current results show that the peak heating and pressure along the second cone occur slightly downstream of reattachment (indicated by the vertical line R).

Unfortunately, a solution that displays qualitative features that are in agreement with experimental findings is not necessarily a good solution, as demonstrated by the present results for the coarser grid simulations. The current DAC simulation must undergo careful comparisons with experimental measurements and other numerical simulations to establish confidence in the results. However, the current findings do suggest that most of the previous G2 solutions presented by the first author for the  $25^\circ/65^\circ$  sharp double cone problem (Refs. [15], [16], and [17], for example) were made with a coarse grid, and the G2 results are qualitative at best for those cases in which the Reynolds number was similar to or higher than that of the current test case.

## CONCLUDING REMARKS

Results of a computational study are presented for Mach 10 air flow about a sharp double cone where the combination of model size and flow conditions produces a significant separated flow region with associated shock/shock and shock/boundary layer interactions. The computations are made with the direct simulation Monte Carlo (DSMC) method by using two codes, the G2 code of Bird and the DAC (DSMC Analysis Code) code of LeBeau. The results presented provide insight into the nature of the shock interactions, their impact on surface quantities, and the sensitivity of the results to computational parameters. Particular emphasis is given to the effects of grid resolution because results from both codes show that the extent of separation grows with increasing grid refinement as the grid-resolved state is achieved. Furthermore, results for the present problem show that it is not practical to achieve a grid-resolved DSMC solution with a scalar code such as G2 but is possible with a parallel code such as DAC.

The calculated extent of separation is quite large for the present problem, with the wetted length of the separated flow exceeding the length of either of the two cones. Opportunities should exist for comparing the current results with experimental measurements for surface heating and pressure distributions, along with the location of separation and reattachment from oil flow measurements.

## ACKNOWLEDGMENTS

The authors acknowledge the assistance of B. Chanetz, T. Pot, and A. Galli of ONERA, Chalais-Meudon, for providing information regarding the model configuration and flow conditions for the tests scheduled in the ONERA R5Ch wind tunnel.

## REFERENCES

1. Holden, M. S., and Wadhams, T. P., "Code Validation Study of Laminar Shock/Boundary Layer and Shock/Shock Interactions in Hypersonic Flow Part A: Experimental Measurements," AIAA Paper 2001-1031, Jan. 2001.

2. Chanetz, B., private communication, ONERA, 92300 Châtillon, France, July 2001.
3. Harvey, J. K., Holden, M. S., and Wadhams, T. P., "Code Validation Study of Laminar Shock/Boundary Layer and Shock/Shock Interactions in Hypersonic Flow Part B: Experimental Measurements," AIAA Paper 2001-1031, Jan. 2001.
4. Gimelshein, S. F., Levin, D. A., Markelov, G. N., Kudryavtsev, A. N., and Ivanov, M. S., "Statistical Simulation of Laminar Separation in Hypersonic Flows: Numerical Challenges," AIAA 2002-0736, Jan. 2002.
5. Moss, J. N., "Hypersonic Flows About a  $25^\circ$  Sharp Cone," NASA/TM-2001-211253, Dec. 2001.
6. Roy, C. J., Bartel, T. J., Gallis, M. A., and Payne, J. L., "DSMC and Navier-Stokes Predictions for Hypersonic Laminar Interacting Flows," AIAA 2001-1030, Jan. 2001.
7. Candler, G. V., Nompelis, I., Druguet, M.-C., Holden, M. S., Wadhams, T. P., Boyd, I. D., and Wang, W. L., "CFD Validation for Hypersonic Flight: Hypersonic Double-Cone Flow Simulations," AIAA Paper 2002-0581, Jan. 2002.
8. Holden, M. S., Wadhams, T. P., Harvey, J. K., and Candler, G. V., "Comparisons Between DSMC and Navier-Stokes Solutions and Measurements in Regions of Laminar Shock Wave Boundary Layer Interaction in Hypersonic Flows," AIAA Paper 2002-0435, Jan. 2002.
9. LeBeau, G. J., "A Parallel Implementation of the Direct Simulation Monte Carlo Method," *Computer Methods in Applied Mechanics and Engineering*, Vol. 174, 1999, pp. 319-337.
10. LeBeau, G. J., "A User Guide for the DSMC Analysis Code (DAC) Software for Simulating Rarefied Gas Dynamic Environments," Revision DAC97-G, NASA Johnson Space Center, Jan. 2002.
11. Bird, G. A., "The G2/A3 Program System Users Manual," Version 1.8, GAB Consulting Pty Ltd, March 1992.
12. Bird, G., *Molecular Gas Dynamics and the Direct Simulation of Gas Flows*, Oxford: Clarendon Press, 1994.
13. Borgnakke, C., and Larsen, P. S., "Statistical Collision Model for Monte Carlo Simulation of Polyatomic Gas Mixture," *Journal of Computational Physics*, Vol. 18, No. 4, 1975, pp. 405-420.
14. Needham, D., and Stollery, J., "Boundary Layer Separation in Hypersonic Flow," AIAA Paper 66-455, Jan. 1966.
15. Moss, J. N., and Olejniczak, J., "Shock-Wave/Boundary-Layer Interactions in Hypersonic External Flows," AIAA Paper 98-2668, June 1998.
16. Moss, J., Olejniczak, J., Chanetz, B., and Pot, T., "Hypersonic Separated Flows at Low Reynolds Number Conditions," *Rarefied Gas Dynamics*, Vol. II, Toulouse: Cepadues-Editions, 1999, pp. 617-624.
17. Moss, J. N., *DSMC Simulations of Shock Interactions About Sharp Double Cones*, NASA/TM-2000-210318, Aug. 2000.

REPORT DOCUMENTATION PAGE			Form Approved OMB No. 0704-0188	
Public reporting burden for this collection of information is estimated to average 1 hour per response, including the time for reviewing instructions, searching existing data sources, gathering and maintaining the data needed, and completing and reviewing the collection of information. Send comments regarding this burden estimate or any other aspect of this collection of information, including suggestions for reducing this burden, to Washington Headquarters Services, Directorate for Information Operations and Reports, 1215 Jefferson Davis Highway, Suite 1204, Arlington, VA 22202-4302, and to the Office of Management and Budget, Paperwork Reduction Project (0704-0188), Washington, DC 20503.				
1. AGENCY USE ONLY (Leave blank)		2. REPORT DATE August 2002		3. REPORT TYPE AND DATES COVERED Technical Memorandum
4. TITLE AND SUBTITLE Hypersonic Shock Interactions About a 25°/65° Sharp Double Cone			5. FUNDING NUMBERS  706-85-42-01	
6. AUTHOR(S) James N. Moss, Gerald J. LeBeau, and Christopher E. Glass				
7. PERFORMING ORGANIZATION NAME(S) AND ADDRESS(ES)  NASA Langley Research Center Hampton, VA 23681-2199			8. PERFORMING ORGANIZATION REPORT NUMBER  L-18199	
9. SPONSORING/MONITORING AGENCY NAME(S) AND ADDRESS(ES)  National Aeronautics and Space Administration Washington, DC 20546-0001			10. SPONSORING/MONITORING AGENCY REPORT NUMBER  NASA/TM-2002-211778	
11. SUPPLEMENTARY NOTES				
12a. DISTRIBUTION/AVAILABILITY STATEMENT Unclassified-Unlimited Subject Category 34      Distribution: Standard Availability: NASA CASI (301) 621-0390			12b. DISTRIBUTION CODE	
13. ABSTRACT (Maximum 200 words) This paper presents the results of a numerical study of shock interactions resulting from Mach 10 air flow about a sharp double cone. Computations are made with the direct simulation Monte Carlo (DSMC) method by using two different codes: the G2 code of Bird and the DAC (DSMC Analysis Code) code of LeBeau. The flow conditions are the pretest nominal free-stream conditions specified for the ONERA R5Ch low-density wind tunnel. The focus is on the sensitivity of the interactions to grid resolution while providing information concerning the flow structure and surface results for the extent of separation, heating, pressure, and skin friction.				
14. SUBJECT TERMS Hypersonic, DSMC, shock/shock interactions, biconic flows			15. NUMBER OF PAGES 13	
			16. PRICE CODE	
17. SECURITY CLASSIFICATION OF REPORT Unclassified	18. SECURITY CLASSIFICATION OF THIS PAGE Unclassified	19. SECURITY CLASSIFICATION OF ABSTRACT Unclassified	20. LIMITATION OF ABSTRACT UL	